Theoretical derivation of flow laws for quartz dislocation creep: Comparisons with experimental creep data and extrapolation to natural conditions using water fugacity corrections

Jun-Ichi Fukuda, Ichiko Shimizu

AGU PUBLICATIONS

JGR

Journal of Geophysical Research: Solid Earth

RESEARCH ARTICLE
10.1002/2016JB013798

Key Points:
- Experimental data, mostly for β-quartz, follow theories with oxygen volume diffusion
- Previous experimental flow laws were modified to include the water fugacity terms
- Pipe-diffusion-controlled dislocation creep dominates under middle crustal conditions

Correspondence to:
J. Fukuda,
jfukuda@eps.s.u-tokyo.ac.jp

Citation:
Fukuda, J., and I. Shimizu (2017), Theoretical derivation of flow laws for quartz dislocation creep: Comparisons with experimental creep data and extrapolation to natural conditions using water fugacity corrections, *J. Geophys. Res. Solid Earth*, *122*, doi:10.1002/2016JB013798.

Received 29 NOV 2016
Accepted 18 JUL 2017
Accepted article online 21 JUL 2017

Theoretical derivation of flow laws for quartz dislocation creep: Comparisons with experimental creep data and extrapolation to natural conditions using water fugacity corrections

Jun-ichi Fukuda[1,2,3,4,5] and Ichiko Shimizu[2]

[1]Department of Geology and Geophysics, Texas A&M University, College Station, Texas, USA, [2]Department of Earth and Planetary Science, The University of Tokyo, Tokyo, Japan, [3]Institut des Sciences de la Terre d'Orléans, UMR 7327, Université d'Orléans, Orléans, France, [4]Now at Department of Earth and Planetary Science, Tokyo University, Tokyo, Japan, [5]Now at Institut des Sciences de la Terre d'Orléans, UMR 7327, Université d'Orléans, Orléans, France

Abstract We theoretically derived flow laws for quartz dislocation creep using climb-controlled dislocation creep models and compared them with available laboratory data for quartz plastic deformation. We assumed volume diffusion of oxygen-bearing species along different crystallographic axes (//*c*, ⊥*R*, and ⊥*c*) of α-quartz and β-quartz, and pipe diffusion of H_2O, to be the elementary processes of dislocation climb. The relationships between differential stress (σ) and strain rate ($\dot{\varepsilon}$) are written as $\dot{\varepsilon} \propto \sigma^3 D_v$ and $\dot{\varepsilon} \propto \sigma^5 D_p$ for cases controlled by volume and pipe diffusion, respectively, where D_v and D_p are coefficients of diffusion for volume and pipe diffusion. In previous experimental work, there were up to ~1.5 orders of magnitude difference in the water fugacity values in experiments that used either gas-pressure-medium or solid-pressure-medium deformation apparatus. Therefore, in both the theories and flow laws, we included water fugacity effects as modified preexponential factors and water fugacity terms. Previous experimental data were obtained mainly in the β-quartz field and are highly consistent with the volume-diffusion-controlled dislocation creep models of β-quartz involving the water fugacity term. The theory also predicts significant effects for the transition of α-β quartz under crustal conditions. Under experimental pressure and temperature conditions, the flow stress of pipe-diffusion-controlled dislocation creep is higher than that for volume-diffusion-controlled creep. Extrapolation of the flow laws to natural conditions indicates that the contributions of pipe diffusion may dominate over volume diffusion under low-temperature conditions of the middle crust around the brittle-plastic transition zone.

1. Introduction

Quartz can largely control the rheology of the continental lithosphere [*Kohlstedt et al.*, 1995; *Behr and Platt*, 2014] and subduction-zone megathrusts [*Shimizu*, 2014] because of its weakness and abundance in crustal material. The development of quartz lattice preferred orientations in ductile shear zones and metamorphic belts indicates the common occurrence of quartz dislocation creep. Until around the middle of the 1990s, the flow law for mineral dislocation creep was expressed as

$$\dot{\varepsilon} = A\sigma^n \exp\left[-\frac{Q_{dis}}{RT}\right], \tag{1}$$

where $\dot{\varepsilon}$ is the strain rate, A is the preexponential factor, σ is the differential stress, n is the stress exponent, Q_{dis} is the activation energy, R is the gas constant, and T is absolute temperature. In the past four decades, many experiments have been performed to determine the flow law parameters of quartz dislocation creep [*Parrish et al.*, 1976; *Jaoul et al.*, 1984; *Kronenberg and Tullis*, 1984; *Koch et al.*, 1989 for older flow laws; *Paterson and Luan*, 1990; *Luan and Paterson*, 1992; *Gleason and Tullis*, 1995; *Rutter and Brodie*, 2004a]. However, there are large variations in the proposed values of n (2–4) and Q_{dis} (120–300 kJ/mol). As a result, when the flow laws are extrapolated to natural temperature conditions, the targeted parameters such as strain rates and flow stresses show variations of more than a few orders of magnitude [e.g., *Wightman et al.*, 2006; *Menegon et al.*, 2011; *Okudaira and Shigematsu*, 2012; *Boutonnet et al.*, 2013].

From the mid-1990s, the effects of water fugacity on plastic deformation, including both dislocation and diffusion creep, had been discussed for quartz [*Gleason and Tullis*, 1995; *Kohlstedt et al.*, 1995; *Post et al.*, 1996;

Hirth et al., 2001; *Rutter and Brodie*, 2004a, 2004b; *Holyoke and Kronenberg*, 2013] and other minerals (e.g., *Mei and Kohlstedt* [2000a, 2000b] and *Karato and Jung* [2003] for olivine, *Hier-Majumder et al.* [2005] for pyroxene, and *Rybacki et al.* [2006] for anorthite). The flow law was then rewritten as

$$\dot{\varepsilon} = A'\sigma^n f_{H_2O}^r \exp\left[-\frac{Q_{dis}}{RT}\right], \quad (2)$$

where the effects of water fugacity, f_{H_2O}, and the water fugacity exponent, r, are separated from the preexponential factor, A'. In addition to water fugacity, contributions of the activation volume V on pressure, as well as the effects of oxygen and hydrogen fugacities, were independently evaluated for olivine and plagioclase [*Karato and Jung*, 2003; *Rybacki et al.*, 2006].

In experiments with strain rates (which generally range from 10^{-3} to 10^{-7} s^{-1}), quartz dislocation creep is known to become dominant at temperatures above ~800°C. When gas-pressure-medium deformation apparatus is used, the maximum confining pressure is ~300 MPa and the α-β transition at 300 MPa takes place at 650°C. Therefore, the temperature conditions that facilitate dislocation creep, when using a gas-pressure-medium deformation apparatus, are always in the β-quartz field. A solid-pressure-medium deformation apparatus generates higher confining pressures of up to ~2 GPa, and the α-β transition occurs at ~800°C at 1.0 GPa and 900°C at 1.5 GPa. Thus, almost all experiments with temperatures that facilitated dislocation creep were performed in the β-quartz field. *Kirby* [1977], *Kirby and McCormick* [1979], and *Linker and Kirby* [1981] and *Linker et al.* [1984] conducted deformation experiments on quartz under atmospheric conditions and reported a change in the temperature dependence of flow stress due to the differences in the activation energies of α-quartz and β-quartz. However, the differences in strengths due to the α-β transition at higher confining pressures have not been clearly observed because of experimental constraints.

In metallography, numerous theoretical creep models have been developed to explain power law creep behavior [*Weertman*, 1955, 1970; *Evans and Knowles*, 1977; *Spingarn et al.*, 1979; *Poirier*, 1985]. *Hirth and Kohlstedt* [2015] used the pipe-diffusion-controlled model to explain olivine dislocation creep, but theoretical considerations for quartz dislocation creep are lacking. For the present study, we compiled experimental data for quartz dislocation creep from the literature in order to evaluate the effects of water fugacity in the form of equation (2) and to constrain the ranges of n and Q_{dis}. Then, we theoretically derived plausible flow laws using material properties such as diffusion constants and compared them with the results of deformation experiments. In this paper we discuss the differences in strength of α-quartz and β-quartz and the contribution of pipe diffusion to dislocation creep. We extrapolate the ranges of pressure and temperature from laboratory to natural conditions, including conditions in the α-quartz stability field and discuss the effects of water fugacity.

2. Empirical Flow Laws of Quartz Dislocation Creep and Corrections for Water Fugacity

Solid-pressure-medium deformation apparatus, such as the Griggs type, take into account the large effects of friction from the rig and the sample assembly on the measured stresses. A correction for friction was not applied in the earlier literature [e.g., *Jaoul et al.*, 1984; *Kronenberg and Tullis*, 1984; *Koch et al.*, 1989], meaning the strength values were imprecise. In addition, *Koch et al.* [1989] reported measured differential stresses in excess of 2 GPa under a confining pressure of 1.0 GPa. *Hirth and Tullis* [1994] experimentally demonstrated that when differential stress exceeds the confining pressure, deformation occurs by semibrittle flow associated with microcrack formation, which is referred to as Goetze's criterion [*Kohlstedt et al.*, 1995]. Therefore, as noted by *Gleason and Tullis* [1995], the experimental results of *Koch et al.* [1989] could be affected by brittle deformation. *Gleason and Tullis* [1995] used a solid-pressure-medium deformation apparatus and a molten salt assembly, which enabled an improved determination of differential stress. Their confining pressure was ~1.5 GPa and temperatures reached 1100°C, with most temperatures in the β-quartz field. The measured differential stresses were <250 MPa, so fracture development by deformation was inhibited. The differential stresses measured by *Gleason and Tullis* [1995] were later corrected by *Holyoke and Kronenberg* [2010]. *Luan and Paterson* [1992] and *Rutter and Brodie* [2004a, 2004b] used gas deformation apparatus, where the stress resolution was thought to be better because of the reduced friction in the gas pressure medium, although the confining pressure was up to a few hundred megapascal. Some of the samples used by *Koch et al.* [1989], *Luan and Paterson* [1992], and *Gleason and Tullis* [1995] included melt

and accessory minerals such as mica, which may have influenced the flow law parameters. In situations where the effects on the experiment of brittle deformation and melt are unlikely, the stress exponents of quartz dislocation creep range from 3 [*Rutter and Brodie*, 2004a] to 4 [*Luan and Paterson*, 1992; *Gleason and Tullis*, 1995]. We suggest therefore that the flow laws used in these three papers, as well as *Holyoke and Kronenberg* [2010], who corrected the stresses given by *Gleason and Tullis* [1995], are the most reliable in terms of stress accuracy and the smallest effects from secondary phases. These flow laws are therefore often applied to natural quartz samples deformed by dislocation creep [*Wightman et al.*, 2006; *Menegon et al.*, 2011; *Okudaira and Shigematsu*, 2012; *Boutonnet et al.*, 2013]. We use the flow laws reported in these four experimental papers. The flow parameters are listed in Table 1. However, *Luan and Paterson* [1992] did not fully explain the procedures used for determining the flow law for quartz aggregates that were prepared from silicic acid, so in this case we used their experimental data and determined the flow law parameters again, as explained in the Appendix A. The stress exponents from their strain rate stepping experiments, as well as all the strain rate-stress relationships, show n = ~3, which is different from their original value of n = 4. We note that most of these previous determinations of flow laws relate to experiments on the plastic deformation of quartz in the β-quartz field.

The activation energies in previous flow laws vary from 152 kJ/mol [*Luan and Paterson*, 1992] to 242 kJ/mol [*Rutter and Brodie*, 2004a], regardless of differences in the stress exponents (Table 1). Our recalculations, using the experimental data of *Luan and Paterson* [1992], show an even smaller activation energy of 121 kJ/mol (Appendix A). *Kronenberg and Tullis* [1984] reported changes in the activation energies from 120 kJ/mol for a sample with 0.4 wt % water added to 300 kJ/mol for a sample heated in a vacuum. The presence of added water, and possibly water already incorporated in the samples, would change the strength and the flow law parameters, although the quantitative effects of such water are unclear. In addition to experimental errors, differences in the flow law parameters might arise from various factors such as differences in starting material and sample assembly, and pressure-temperature conditions. Because quartz has several slip systems and their activities are largely dependent on pressure and temperature [*Lister et al.*, 1978; *Lister*, 1981; *Takeshita and Wenk*, 1988], different slip systems may be governed by different flow laws.

The contribution of water fugacity to the quartz flow law was not explicitly given until the 2000s. We will therefore determine A' for each flow law. For the fugacity exponent of r, some researchers reported variations in quartz dislocation creep for r values between ~0.4 and 2.8, which were obtained from the ratio of r/n with n = ~4 [*Paterson*, 1989; *Gleason and Tullis*, 1995; *Post et al.*, 1996; *Chernak et al.*, 2009; *Holyoke and Kronenberg*, 2013]. We applied the water fugacity exponent value of r = 1, as demonstrated by *Gleason and Tullis* [1995], and which was also applied for the sake of simplicity by *Rutter and Brodie* [2004a]. *Kohlstedt et al.* [1995] used the experimental data of *Kronenberg and Tullis* [1984] and obtained a similar r value. To calculate water fugacity, we used the molar volume and the equation of state for pure water given by *Pitzer and Sterner* [1994] and *Sterner and Pitzer* [1994], respectively. Using a representative value of water fugacity for the range in pressure and temperature for each experiment (*f_{H_2O} in Table 1), A' was determined as

$$A' = A/{}^{*}f^{r}_{H_2O}. \tag{3}$$

The calculated A' values for previous flow laws are given in Table 1. It should be noted that the calculation of *f_{H_2O} assumed pore fluids that were saturated with pure water. However, *Hirth et al.* [2001] suggested that the experiments by *Gleason and Tullis* [1995] might have been conducted under water-undersaturated conditions, and *Shimizu* [2008] pointed out that the pore fluids in the experiments by *Rutter and Brodie* [2004a] may also not have been pure water as a result of redox reactions occurring between the sample and the iron jacket. Thus, the calculated *f_{H_2O} values in these experiments may have been overestimated (i.e., A' was underestimated).

In addition to using the experimental data for dislocation creep given by *Luan and Paterson* [1992] and *Gleason and Tullis* [1995], *Hirth et al.* [2001] used microstructural information on naturally deformed quartzite and proposed the following optimum values for flow law parameters: $\log A' = -11.2$ MPa^{-n-r} s^{-1}, n = 4, Q_{dis} = 135 kJ/mol, and r = 1. Although the flow law proposed by *Hirth et al.* [2001] has been frequently applied to naturally deformed quartz, some of their assumptions are uncertain. First, to determine the paleo-stress from the microstructures of natural quartzite, they directly extended the use of the grain-size piezometer to low-grade metamorphic conditions (the piezometer had been calibrated by *Twiss* [1977] for laboratory

Journal of Geophysical Research: Solid Earth

10.1002/2016JB013798

Table 1. Flow Law Data and Experimental Conditions[a]

No.	Ref.	Quartz Aggregate Sample	Water Cont ppm H_2O	Apparatus	*Pc*, *T*, Corresponding fH_2O (*Applied fH_2O)	Log *A* ($MPa^{-n}\ s^{-1}$)	Log *A′* ($MPa^{-n-r}\ s^{-1}$)	*n*	Q_{dis} (kJ/mol)	Remarks
1	*Luan and Paterson* [1992] (L&P92)	Crystallization from silicic acid	30–1000 (intra + gb)	Gas	0.3 GPa, 827–1027°C, 0.25–0.3 GPa (*280 MPa)	−9.40	*−11.85*	4 ± 0.8	152 ± 71	Water content determination by IR with the *Paterson* [1982]'s calibration
2	Revised *Luan and Paterson* [1992] (L&P92Rev)					*−7.20 ± 0.52*	*−9.65*	*3*	*121 ± 13*	See Appendix for the determination
3	*Gleason and Tullis* [1995] (G&T95)	Black Hill quartzite (no melt)	1500 (intra + gb)	Solid	~1.5 GPa, 900–1100°C, 5.0–5.2 GPa (*5100 MPa)	−3.96 ± 1.96	*−7.67*	4 ± 0.9	223 ± 56	Water content determination by thermogravimetry + IR (Calibration unclear)
4	Revised *Gleason and Tullis* [1995] in *Holyoke and Kronenberg* [2010] (G&T95 + H&K10)					−3.29	*−7.00*			
5	*Rutter and Brodie* [2004a] (R&B04)	Brazilian quartz powder + Hot press	1.5–3.0 (intra) <1000 (gb)	Gas	0.3 GPa, 1100–1200°C, 0.31–0.32 Ga (*300 MPa)	−2.45 ± 0.39	−4.93	2.97 ± 0.39	242 ± 24	Water content by IR for intracrystalline water. (Calibration unclear) and thermogravimetry for powder including adsorbed water.

[a]For the fugacity correction, the fugacity exponent *r* was set at 1. See the applied $*f_{H_2O}$ and the explanation in the text. Available errors are shown. The italicized values were determined during our study. All experimental conditions are in the β-quartz field.

data), even though it had been predicted theoretically that recrystallized grain size would be affected substantially by temperature [e.g., *de Bresser et al.*, 1998, 2001; *Shimizu*, 1998]. The calculation for quartz indicates that in agreement with laboratory observations [*Stipp and Tullis*, 2003; *Stipp et al.*, 2006], the temperature dependence of the piezometric relation is negligible at temperatures above 800°C. However, this temperature dependence becomes considerably more important under the conditions of the middle crust [*Shimizu*, 2008, 2012]. They also used the regime 2–3 boundary of *Hirth and Tullis* [1992] as a constant stress line and extended its use to recrystallization microstructures formed on geologic time scales; however, there is no physical basis for assuming that the microstructural boundary only depends on differential stress. Second, the strain rate during thrust movements of sheets of quartzite, as estimated using geochronological methods, is the minimum strain rate, because deformation would not necessarily occur continuously over the entire duration of an orogeny. In this case, the strain rate that directly changes the quartzite flow becomes larger. Thus, the determination of these flow law parameters in natural shear zones could be biased by uncertainties in $\dot{\varepsilon}$-σ conditions. In this paper we focus on experimental data and do not discuss semiempirical treatments such as those of *Hirth et al.* [2001].

3. Climb-Controlled Dislocation Creep Model of Quartz

A strain rate that is controlled by dislocation climb associated with volume diffusion is generally written [e.g., *Weertman*, 1955, 1970; *Evans and Knowles*, 1977; *Spingarn et al.*, 1979; *Poirier*, 1985] in the form of

$$\dot{\varepsilon}_v = X\frac{\mu b}{kT}\left(\frac{\sigma}{\mu}\right)^n D_v, \tag{4}$$

where X is a nondimensional factor, k is the Boltzmann constant (1.381×10^{-26} kJ/mol), and D_v is the volume diffusion coefficient ($m^2\ s^{-1}$). The shear modulus μ of quartz is 42×10^3 MPa. The Burgers vector depends on the slip system, but it is associated with the unit cell of quartz [*Baëta and Ashbee*, 1969; *Epelboin and Patel*, 1982; *Mainprice et al.*, 1986]. We therefore used 5×10^{-10} m for simplicity. According to the model of *Spingarn et al.* [1979], the constant X is set at 1 and a stress exponent of 3 is applied. Different models have been proposed with different values of X and n, with $X = 0.01$–100 and $n = 3$–5 for the climb-controlled model [*Weertman*, 1955, 1970; *Evans and Knowles*, 1977]. In this paper we start with the simple model of *Spingarn et al.* [1979] where the stress exponent is close to that obtained in quartz creep experiments. *Platt and Behr* [2011] theoretically derived a quartz flow law accompanied by dynamic recrystallization, which includes a grain size exponent of 1 and a stress exponent of 3 or 4. They used scaling factors on the order of ~10^{-7} to match their parameters with experimental data. However, refining experimental and theoretical data is not the purpose of our study, so we do not use any scaling factors.

The variable parameter which changes the order of strain rate is the volume diffusion coefficient. *Giletti and Yund* [1984] and *Farver and Yund* [1991] determined the volume diffusion coefficients of oxygen-bearing species for α-quartz and β-quartz. The activation energies are 120–280 kJ/mol, depending mainly on the crystallographic orientation and quartz phase. These values are similar to the activation energies for quartz dislocation creep, as reported previously (Table 1). *Béjina and Jaoul* [1996] determined silicon volume diffusion coefficients parallel to the *c* axis in the β-quartz field under atmospheric conditions and a confining pressure of 2 GPa. The activation energy for silicon diffusion is ~750 kJ/mol, which is much higher than for quartz dislocation creep. The activation energy of silicon diffusion does not depend on confining pressure, and hence, it also does not depend on water fugacity. Thus, the proposed diffusing species is the Frenkel defect of silicon, which does not involve hydrogen, meaning there is no dependence on water fugacity. In the case of olivine, the activation of silicon diffusion is consistent with dislocation creep experiments [e.g., *Kohlstedt*, 2006] and has the potential to explain experimental data [*Hirth and Kohlstedt*, 2015]. Silicon volume diffusion may operate in the case of silicate structures where the silica tetrahedra are isolated or not fully connected in three dimensions, but it may not be valid for a framework silicate such as quartz.

Thus, we used the oxygen-bearing diffusion data of *Giletti and Yund* [1984] and *Farver and Yund* [1991]. In their diffusion experiments, they doped the quartz with $H_2{}^{18}O$ and traced the ^{18}O profile with an ion microprobe. These authors argued that the possible diffusing species were O_2, H_2O, H_3O^+, and/or O^{2-}. They also demonstrated the dependence of the diffusion coefficients on water fugacity, and they obtained a fugacity exponent of ~1. These results show therefore that the volume diffusion of oxygen-bearing species is probably

Table 2. Diffusion Data Used for the Dislocation Creep Theories[a]

	Volume Diffusion Oxygen-Bearing Species				Pipe Diffusion Precipitation of H_2O Clusters
	Giletti and Yund [1984]		*Farver and Yund* [1991]		*Cordier et al.* [1988]
Phase	α-quartz	β-quartz	α-quartz	Phase	α-quartz, β-quartz
Expt temp range °C	500–550	600–800	450–590	Expt temp range °C	350–1000
Corresponding fH_2O (MPa) at Pc = 100 MPa (Applied value)	46–56 (50)	77–86 (80)	36–62 (50)	Confining pressure (MPa)	atom—700 (No pressure ~ fugacity effect and no phase effect)
	//c (Brazilian) 1 ppm H_2O				(Synthetic) 60 ppm H_2O
D_{v0} m^2 s^{-1}	1.9×10^{-2}	$4\ (+3, -2) \times 10^{-11}$	2.9×10^{-5}	D_{p0} m^2 s^{-1}	10^{-12}
D'_{v0} m^2 s^{-1} MPa^{-1}	3.8×10^{-4}	5.0×10^{-13}	5.8×10^{-7}	Q_p kJ/mol	95
Q_v kJ/mol	284 ± 92	142 ± 4	243 ± 17		
	⊥R (Brazilian)			Comment	Observation on (0001)
D_{v0} m^2 s^{-1}	$8\ (+50, -7) \times 10^{-6}$	$9\ (+21, -7) \times 10^{-11}$	–		
D'_{v0} m^2 s^{-1} MPa^{-1}	1.6×10^{-7}	1.1×10^{-12}	–		
Q_v kJ/mol	238 ± 12	155 ± 8	–		
	⊥c (Brazilian)				
D_{v0} m^2 s^{-1}	–	$1\ (+2, -1) \times 10^{-8}$	–		
D'_{v0} m^2 s^{-1} MPa^{-1}	–	1.3×10^{-10}	–		
Q_v kJ/mol	–	234 ± 8	–		
	⊥c (Synthetic; X-507) 55 ppm H_2O				
D_{v0} m^2 s^{-1}	–	$2\ (+9, -2) \times 10^{-10}$	–		
D'_{v0} m^2 s^{-1} MPa^{-1}	–	2.5×10^{-12}	–		
Q_v kJ/mol	–	205 ± 8	–		

[a]Available errors are shown. For the fugacity correction, see the applied $*f_{H_2O}$ and the explanation in the text.

the rate-limiting process of quartz dislocation creep. If the diffusion of molecular water is the rate-limiting process, the hydrolytic weakening of framework silicates such as quartz is possible [e.g., *Griggs and Blacic*, 1965; *Griggs*, 1974; *Kirby*, 1977; *Kronenberg and Tullis*, 1984]. The diffusion coefficients in these papers were given as the Arrhenius relation:

$$D_v = D_{v0} \exp\left(-\frac{Q_v}{RT}\right), \tag{5}$$

where D_{v0} is the preexponential factor (m^2 s^{-1}), Q_v is the activation energy of volume diffusion (kJ/mol), R is the gas constant, and T is absolute temperature. *Farver and Yund* [1991] showed the water fugacity exponent to be ~1, and their Arrhenius relation is given as equation (5). For our study therefore we determined D_{v0}' (m^2 s^{-1} MPa^{-r}) using the following equation, which includes the water fugacity term (r = 1) and is similar to equation (3):

$$D_{v0}{}' = D_{v0}/{}^*f^r_{H_2O}. \tag{6}$$

The diffusion coefficients differ for different crystallographic directions in α-quartz and β-quartz, as summarized in Table 2. Unfortunately, because of the low diffusion coefficients, there are no diffusion data for the direction perpendicular to the c axis in α-quartz. In this paper we use equations (4)–(6) to calculate the theoretical flow law of dislocation creep in quartz using volume diffusion coefficients for oxygen-bearing species along the different crystallographic directions in α-quartz and β-quartz.

Strain rates controlled by dislocation climb through pipe diffusion were theoretically calculated by *Spingarn et al.* [1979], and they gave the flux balance of substances between dislocation cores and circumferences in terms of volume diffusion. In another approach, they also assumed that local climb of the dislocation core took place only by pipe diffusion. In these two cases, the following equation can be obtained, which is similar to equation (4):

$$\dot{\varepsilon}_p = Y \frac{\mu b}{kT} \left(\frac{\sigma}{\mu}\right)^{n'} D_p. \tag{7}$$

Y is a nondimensional factor, assigned a value of 18, which is derived from a standard dislocation climb distance and the density of an impurity (water clusters in the present study) via pipe diffusion. D_p is the pipe diffusion coefficient ($m^2\ s^{-1}$), which is expressed using the preexponential factor D_{p0} and the activation energy Q_p (kJ/mol) as follows:

$$D_p = D_{p0} \exp\left(-\frac{Q_p}{RT}\right). \tag{8}$$

The stress exponent n' is 5. In the experimental deformation of some metals, observations of power law creep with an exponent of 5 have been interpreted to reflect the contribution of pipe diffusion to dislocation climb [*Luthy et al.*, 1980; *Ruano et al.*, 1981; *Huang et al.*, 2002; *Mathew et al.*, 2005; *Somekawa et al.*, 2005]. However, the dominance of dislocation creep controlled by pipe diffusion has not been directly verified and the occurrence of pipe diffusion was only recently demonstrated by *Legros et al.* [2008] for silicon diffusion in aluminum.

Cordier et al. [1988] analyzed the traveled distance of water clusters in quartz, assuming precipitation and growth through pipe diffusion, and concluded that the pipe diffusion coefficients for α-quartz and β-quartz follow a single Arrhenius relation, indicating the absence of a phase effect. We used the pipe diffusion coefficients of quartz given by *Cordier et al.* [1988]. Pipe diffusion in quartz is considered to involve an exchange reaction between SiO_2 and H_2O through dislocations that are connected by freezable and/or nonfreezable molecular water clusters [*Trepied and Doukhan*, 1978; *Cordier et al.*, 1988; *Kronenberg*, 1994]. If this exchange reaction rate is controlled by H_2O diffusion, it would demonstrate a dependency on water fugacity.

4. Comparisons Between Creep Data and Theoretical Models

We compared the experimental data with theories for quartz dislocation creep that are available in the literature. With respect to the theories, we used equation (6) to apply water fugacity, as calculated from the pressure and temperature for each experimental condition [*Pitzer and Sterner*, 1994; *Sterner and Pitzer*, 1994]. The water fugacity values range up to 5.2 GPa for experimental data obtained using solid-pressure-medium (Griggs-type) apparatus, where the pressure–temperature conditions are up to 1.5 GPa and 1100°C. We used the experimental data obtained by *Gleason and Tullis* [1995] and *Stipp and Tullis* [2003], who used Griggs-type apparatus and molten salt assemblies. One data point from *Stipp and Tullis* [2003] at 700°C was taken from an experiment using a solid salt assembly. Their stress data were corrected according to the relationship provided by *Holyoke and Kronenberg* [2010]: $\sigma_{true} = \sigma_{measured} \times 0.73$ for a molten salt assembly and $\sigma_{true} = \sigma_{measured} \times 0.73$–48 for a solid salt assembly. The diffusion data for oxygen-bearing species reported by *Giletti and Yund* [1984] and *Farver and Yund* [1991] were obtained under water fugacities of ~50–80 MPa (Table 2), whereas water fugacities in the creep experiments using a Griggs-type deformation apparatus are up to 2 orders of magnitude higher. As we show below, without applying the water fugacity correction to the theories, none of these experimental data match any of the theories when a Griggs-type deformation apparatus is used. As discussed by *McLaren et al.* [1989], work-hardening is not likely at the high-temperature experiments, and in fact, in all the experiments listed in Table 1, no significant work-hardening process was seen in the mechanical data.

Figure 1 shows the results of comparing the experimental creep data with the theories. In the experimental pressure and temperature conditions of the β-quartz field, the theoretical lines for α-quartz are based on calculations and are not realistically stable (or vice versa). Deformation experiments for α-quartz are limited, since temperatures in the stability field of α-quartz are too low for plastic deformation to occur under laboratory conditions. On the other hand, differences in the strength of α-quartz and β-quartz have been reported at high temperatures and atmospheric pressure conditions [*Kirby*, 1977; *Kirby and McCormick*, 1979; *Linker and Kirby*, 1981; *Linker et al.*, 1984]. According to those results, when the strain rate-temperature relationship under a given differential stress (e.g., ~140 MPa) for α-quartz is extrapolated to the β-quartz field, the strain rate of α-quartz becomes a few orders of magnitude higher than that for β-quartz. This outcome is predicted by the comparisons of the experimental data with the theories (Figure 1).

The strain rate–stress data reported by *Luan and Paterson* [1992] are generally close to the theoretical lines for $\perp R$ and $//c$ in β-quartz (Figure 1a). The temperature-stress relationship is also similar to the line for $\perp R$ in

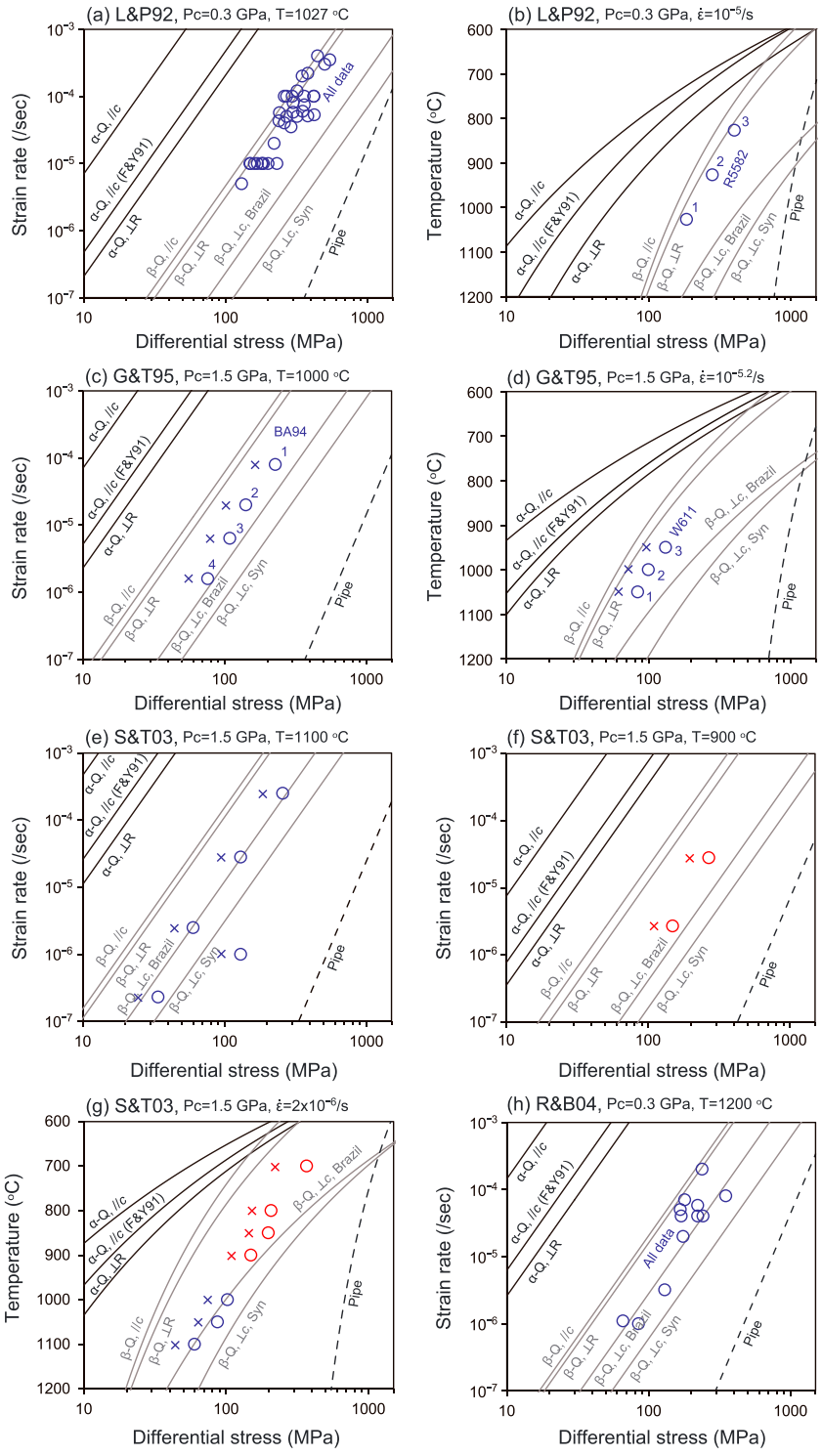

Figure 1. Comparisons of experimental data with theory. (a, c, e, f, and h) Strain rate-stress relationships. (b, d, and g) Temperature-stress relationships. F&Y91 = *Farver and Yund* [1991], L&P92 = *Luan and Paterson* [1992], G&T95 = *Gleason and Tullis* [1995], S&T03 = *Stipp and Tullis* [2003], R&B04 = *Rutter and Brodie* [2004a]. Data for α-quartz and β-quartz are shown with red and blue circles, respectively. Stress data obtained from a solid-pressure-medium (Griggs-type) deformation apparatus were corrected by *Holyoke and Kronenberg* [2010] and are shown as cross symbols. Experimental numbers are shown for some of the data from the earlier literature. Single numbers show procedures in strain rate or temperature stepping experiments. The black lines for α-quartz and the gray lines for β-quartz are theoretical lines calculated using equation (4) with diffusion coefficients for different crystallographic orientations. The black dashed lines were calculated for pipe diffusion using equation (7). See Table 2 for the diffusion data and samples.

β-quartz (Figure 1b), indicating a similarity in the activation energies (155 kJ/mol for the theory and 121 kJ/mol on average with $n = 3$ for the revised experimental data of *Luan and Paterson* [1992] (Appendix A)). The experimental data obtained when using a Griggs-type deformation apparatus are distributed within the theoretical lines for β-quartz (Figures 1c–1g). In contrast, the temperature-stress relationship for α-quartz given by *Stipp and Tullis* [2003] deviates from the theoretical trend for β-quartz (Figure 1g) and also appears to be inconsistent with theoretical predictions for α-quartz. More experimental creep data are needed in the α-quartz field to verify changes in flow law parameters at the α-β transition, as addressed by the creep experiments under atmospheric conditions of *Kirby* [1977], *Kirby and McCormick* [1979], and *Linker and Kirby* [1981] and *Linker et al.* [1984]. Differences in strength also exist between α-quartz and β-quartz under high confining pressures. *Rutter and Brodie* [2004a] used dry Brazilian quartz in their deformation experiments, as also used in the oxygen diffusion experiments of *Giletti and Yund* [1984] and *Farver and Yund* [1991]. The creep data given by *Rutter and Brodie* [2004a] are close to the theoretical values for $\perp c$ near the lowest strain rate of $10^{-6.0}$ s^{-1} (Figure 1h), but with increasing strain rate the creep data approach the theoretical curves for $\perp R$ and $//c$. The authors also measured the crystallographic orientations of quartz after the experiments, and they analytically showed that while basal $<a>$ slip dominated, all slip systems could have accommodated the imposed strain. There are no rigorous explanations to link the diffusion direction of the oxygen-bearing species with the slip system: diffusion $//c$ can be the rate-limiting process even for basal $<a>$ slip, where dislocation glide parallel to $<a>$ occurs readily and climb $//c$ is the rate-limiting process. As shown for olivine, transitions in the slip systems that are operating may be associated with water content [*Jung et al.*, 2006], but the relationship with a theoretical approach is unclear [*Hirth and Kohlstedt*, 2015].

Figure 1 shows, among other data, the flow stresses calculated for the pipe-diffusion-controlled dislocation creep model. Since volume diffusion and pipe diffusion are concurrent processes, and both contribute to dislocation climb, the total strain rate is expressed as the sum of $\dot{\varepsilon}_v$ and $\dot{\varepsilon}_p$. Where one is much higher than the other, the total deformation is controlled by the faster mechanism, whereas under a constant strain rate the weaker mechanism dominates. For most of the β-quartz experimental conditions shown in Figure 1, the flow stresses calculated for volume-diffusion-controlled creep are smaller than those for pipe-diffusion-controlled creep, particularly at temperatures higher than 900°C. Hence, theory predicts the dominance of volume-diffusion-controlled recovery creep with a stress exponent of 3 under laboratory conditions. In all of Figure 1, the experimental data for β-quartz and theoretical curves for different volume-diffusion directions are similar within 1 order of magnitude, although the differences become larger when they are extrapolated to natural conditions as shown in the next section. Volume diffusion in a crystal can occur in all directions. Thus, the actual strain rate of the volume-diffusion-controlled creep would be a weighted average of the theoretical curves that assume diffusion along specific crystallographic axes. As $//c$ and $\perp c$ are the fastest and slowest directions in β-quartz, respectively, flow stresses smaller than the $\perp c$ curve and slightly larger than the $//c$ curve are theoretically expected. In Figure 1, the experimental data of *Luan and Paterson* [1992] and the corrected data of *Gleason and Tullis* [1995] are strikingly similar to this theoretical prediction (Figures 1a–1d), despite the large difference in confining pressure of the original experimental data sets (Table 1). This result supports the inference that the rate of high-temperature dislocation creep in quartz is controlled by recovery processes associated with the volume diffusion of oxygen-bearing species. It also means that the diffusivity of these species is influenced by water fugacity. The experimental data of *Stipp and Tullis* [2003], except for the data point at the lowest temperature (700°C), were obtained with the same apparatus and experimental procedures as those of *Gleason and Tullis* [1995], and their β-quartz data (Figure 1e) show a similar trend to that of *Gleason and Tullis* [1995] in Figure 1e except for the data at $\dot{\varepsilon} = 10^{-6}$ s^{-1}. Some of the results of *Rutter and Brodie* [2004a] (Figure 1h) plot outside the theoretically plausible range, even though their experiments were conducted at the same confining pressure as those of *Luan and Paterson* [1992]. This effect may be related to the very low intracrystalline water content of the starting material (Brazilian quartz; Table 1). In other words, the water-undersaturated pore fluid may have resulted in less pronounced weakening effects than would be expected based on the calculated value of f_{H_2O}.

The creep mechanism discussed above is consistent with the elementary processes of quartz deformation inferred from dynamic recrystallization theory. Assuming that the subgrain rotation (SGR) nucleation rate is controlled by volume-diffusion-associated dislocation climb, *Shimizu* [1998, 2008, 2011] derived the stress exponent, p, of recrystallized grain size during continuous dynamic recrystallization. This theoretical prediction ($p = 1.25$–1.33) corresponds with an experimentally determined value ($p = 1.26$) for quartzite dislocation

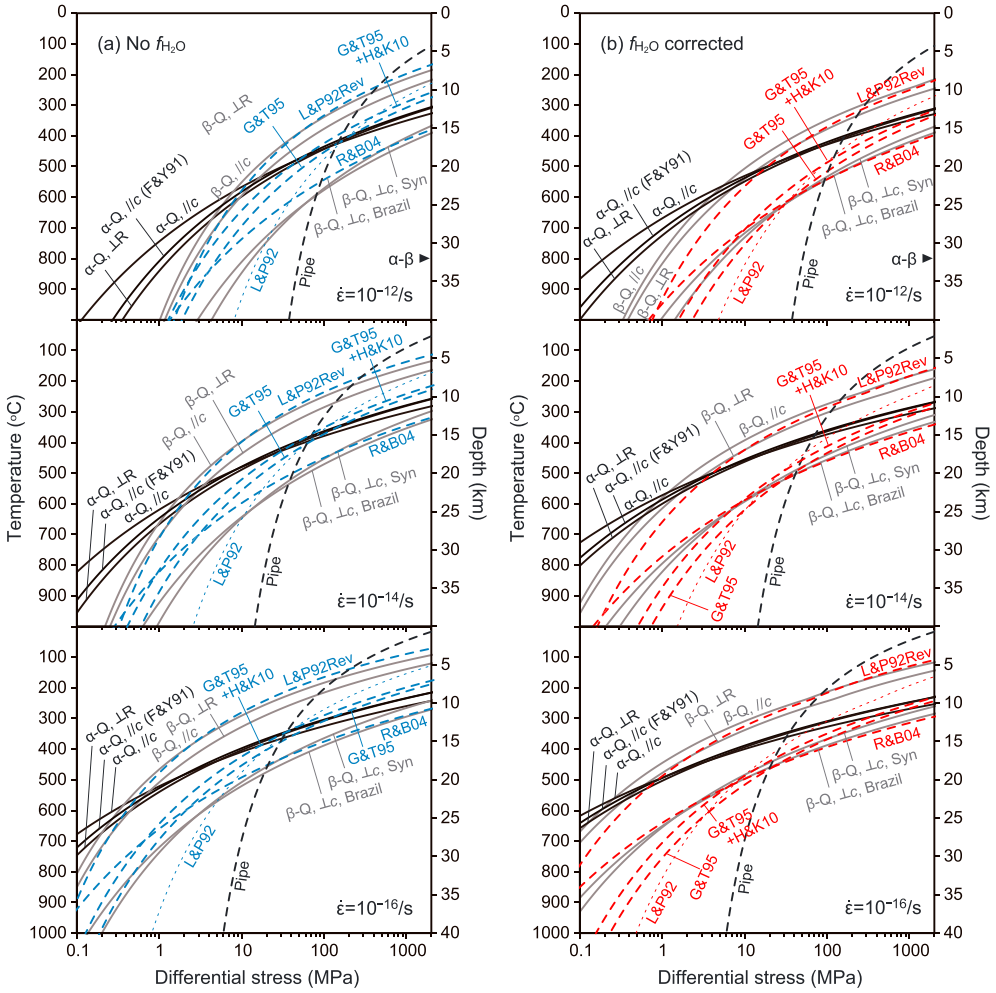

Figure 2. Flow strength of quartz in the continental crust calculated for three geological strain rates. Temperature and pressure gradients are 25°C/km and 27 MPa/km, respectively. The α-β transition is shown by an arrow. The theoretical lines for α-quartz and β-quartz and pipe diffusion, constructed from diffusion data in Table 2, are shown by solid black, solid gray, and black dashed lines, respectively. (a) No water fugacity corrections applied to theoretical or experimental (blue) flow laws. (b) Both theoretical and experimental (red) flow laws include corrections for water fugacity. See Table 1 and caption of Figure 1 for the experimental flow laws and abbreviations.

creep regimes 2 and 3 [*Stipp and Tullis*, 2003], for which recrystallization mechanisms were classified into continuous dynamic recrystallization with "SGR" and "SGR plus grain boundary migration," respectively [*Shimizu*, 2008, section 3.3]. Furthermore, calculations using the diffusion of oxygen-bearing species in the *//c* direction of β-quartz [*Shimizu*, 2012] yield piezometric relations that are close to the empirical piezometer after applying the friction correction of *Holyoke and Kronenberg* [2010].

5. Extrapolation to Natural Conditions

We have extrapolated the theoretical and experimentally determined flow laws to natural conditions. Figure 2 shows the flow strength of quartz under crustal conditions at strain rates of 10^{-12}, 10^{-14}, and 10^{-16} s^{-1}. The temperature and pressure gradients are set at 25 °C/km and 27 MPa/km, respectively. Using these temperature and pressure gradients, the water fugacity was calculated from the equation of state for pure water [*Pitzer and Sterner*, 1994; *Sterner and Pitzer*, 1994]. We used equations (4) and (7) for theoretical quartz dislocation creep controlled by volume diffusion and pipe diffusion, respectively. We corrected the experimental flow laws with equation (3) if the water fugacity term was not given in the original papers (Table 1). Water fugacity is not included in either the theoretical or experimental flow laws in Figure 2a,

but it is included in Figure 2b. The pressure and temperature conditions in Figure 2 are mostly in the α-quartz field, and the data for β-quartz are based on calculations.

For all strain rates, the water-fugacity-corrected flow laws derived from the experiments show trends similar to the theoretical lines for β-quartz (Figure 2b). As is the case for their raw experimental data (Figures 1a and 1b), the revised flow laws of *Luan and Paterson* [1992] are close to the theoretical lines for //*c* and ⊥*R*. The original flow law of *Gleason and Tullis* [1995] did not include a water fugacity term, but when this flow law is corrected for water fugacity, the experimental flow law for β-quartz roughly coincides with the theoretical line for β-quartz ⊥*c*. In general, activation energies and preexponential factors result in a large change in the order of magnitude of the strain rate. In experiments, preexponential factors were determined simply to adjust the experimental data. Nevertheless, the differences in the flow strength of β-quartz calculated from theories and flow laws that include the water fugacity term are within 1 order of magnitude over the wide range of temperatures shown in Figure 2b. This is a consequence of the fact that the theoretical parameter settings, including activation energy (n = 3, Q_v = 142–234 kJ/mol; Table 2), largely overlap with those of the empirical parameters (n = 3–4, Q_{dis} = 121–242 kJ/mol; Table 1). The relation between the flow strength and the water contents listed in Table 1 is not evident. However, in the temperature stepping experiment of *Luan and Paterson* [1992], the sample with higher water content showed a lower activation energy than the sample with less water (Appendix A), indicating the strong influence of H_2O. The flow strength of β-quartz could differ from that of α-quartz (Figures 1 and 2), as inferred from theory and uniaxial compression experiments with highly accurate stress measurements [e.g., *Kirby*, 1977], as mentioned above. Caution is needed therefore when experimentally determined flow laws for β-quartz are applied to naturally deformed α-quartz.

The theory of *Spingarn et al.* [1979] considered dislocation creep that was controlled by pipe diffusion with a stress exponent of n = 5. This type of dislocation creep has not been confirmed under experimental conditions of quartz (Figure 1), but under natural conditions (Figure 2) dislocation creep controlled by pipe diffusion may dominate over dislocation creep controlled by volume diffusion for α-quartz at temperatures around 300°C. The strength of the middle crust calculated from volume-diffusion-controlled creep of α-quartz is extremely high (σ = ~1 GPa) at the lower temperature limit of plastic deformation (~300°C). In contrast, if pipe-diffusion-controlled creep dominates, the middle crustal strength at similar temperatures is reduced to 50–300 MPa. The phase transition of quartz would not affect the flow law of pipe-diffusion-controlled creep, because there are no differences in the pipe diffusion coefficients of α-quartz and β-quartz [*Cordier et al.*, 1988].

The piezometric relations of dynamically recrystallized grain size obtained for regimes 2 and 3 of quartzite deformation [*Stipp and Tullis*, 2003] are consistent with the dislocation creep model that considers dislocation climb by diffusion of oxygen-bearing species as discussed in the previous section. Quartzite deformation and recrystallization microstructures under the high-temperature/low strain rate conditions that correspond to regimes 2 and 3 are characterized by recovered dislocation substructures and SGR nucleation [*Hirth and Tullis*, 1992], which are typical of continuous dynamic recrystallization [*Shimizu*, 2008]. Since free dislocation density is low in regimes 2 and 3, pipe diffusion would not be an important elementary process of dislocation climb. In contrast, under the low-temperature/high strain rate conditions of regime 1, *Hirth and Tullis* [1992] reported numerous free dislocations and only limited recrystallization associated with grain boundary bulging (BLG), a characteristic of discontinuous dynamic recrystallization (DDRX). The grain size stress exponent in regime 1 (p = 0.61 after *Stipp and Tullis* [2003]) deviates from that of the theoretical model for continuous dynamic recrystallization [*Shimizu*, 2008]. It is therefore possible that volume-diffusion-controlled dislocation creep is not the dominant mechanism in regime 1 and that pipe diffusion may play an important role. Moreover, microstructural transitions similar to regimes 1–3 of *Hirth and Tullis* [1992] have been described from naturally deformed quartz rocks [*Hirth et al.*, 2001; *Stipp et al.*, 2002a, 2002b]. Mylonitic vein quartz studied by *Stipp et al.* [2002a, 2002b] exhibits regime 1 and 2 transition (i.e., BLG/SGR transition in their terminology) at the metamorphic temperature approximated by the ~400°C isograd. This temperature is similar to the cross-over temperature of pipe- and volume-diffusion-controlled creep for α-quartz (Figure 2b). It is therefore possible that a change in the dislocation creep mechanism could be linked with the deformation and recrystallization microstructures of quartz.

In Figure 3, fugacity-corrected experimental flow laws for quartz are compared with theoretically derived flow laws using a linear stress scale. Frictional strengths of typical fault zones are also shown for reference. A modified Byerlee's law for ordinary rocks and minerals under hydrothermal conditions, as proposed by

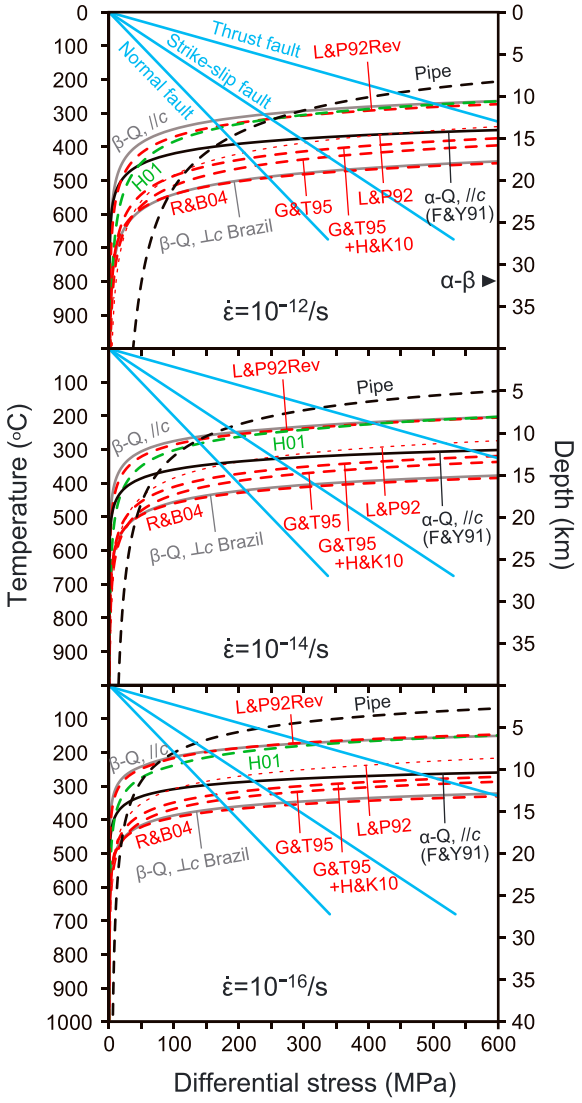

Figure 3. Estimates of the strength of quartz under deformation conditions appropriate to the continental crust. The light blue lines show frictional strengths of fault zones calculated with a modified Byerlee's law for hydrothermal conditions [*Shimizu*, 2014]. Most optimally oriented faults in the continental crust, which has a density of 2.75 g/cm^3 and a hydrostatic pore pressure gradient, are assumed faults. For strike-slip faults, the mean principal stress is taken to be the same as the vertical stress. For the lower part of the diagrams, representative flow laws of quartz in Figure 2 are replotted using a linear stress scale. Both theoretical and experimental flow laws include corrections for water fugacity. H01 = *Hirth et al.* [2001]. Other physical parameters, line colors, and abbreviations follow Figures 1 and 2b.

Shimizu [2014], with a coefficient of friction of 0.7 at effective normal stresses less than 500 MPa, was used for the frictional law. Excess pore pressures and the presence of mica and clay minerals may reduce the fault strength. Flow stresses of β-quartz derived from previous experimental flow laws intersect frictional strengths at unrealistically high stresses for thrust faults and rather high brittle-plastic transition temperatures (~400°C) for normal faults. The revised flow law of *Luan and Paterson* [1992] and theoretical flow law for β-quartz give much smaller stress values, although extrapolation of these flow laws into the α-quartz stability field in nature is not theoretically justified, as discussed above. The volume-diffusion-controlled model of α-quartz gives extremely high stresses at the onset of dislocation creep of quartz at around 300°C, which is considered as the temperature of the brittle-plastic transition for quartz rocks [e.g., *Behr and Platt*, 2014]. The theoretical prediction of pipe diffusion likely explains the crustal strength at the upper end of the plastic deformation regime. Figure 3 also shows the flow stresses calculated using the semiempirical relation proposed by *Hirth et al.* [2001]. Their stress estimates for natural deformation conditions were based on the grain-size piezometer of *Twiss* [1977], as mentioned above. At low temperatures (300–400°C), the flow law by *Hirth et al.* [2001] gives much lower stresses than those represented by the envelopes of volume-diffusion-controlled and pipe-diffusion-controlled dislocation creep of α-quartz. It is likely that the Twiss piezometer considerably underestimates the differential stress in nature as predicted by dynamic recrystallization theories [e.g., *Shimizu*, 2011].

The theoretical model of pipe-diffusion-controlled creep seems to satisfactorily explain the strength of the middle crust and is also consistent with the microstructural transition that occurred around 400°C, as discussed above. However, the occurrence of pipe-diffusion-controlled creep cannot, as was the case for metals, be easily confirmed by observations of dislocations. The relationship between microstructural changes and flow laws has not been experimentally verified, largely due to the difficulty of accurately measuring stress in dislocation creep regime 1 [e.g., *Stipp and Tullis*, 2003]. Thus, the operation of other creep mechanisms also needs to be considered in explanations of middle crustal strength. For example, the occurrence of DDRX,

which is accompanied by strain-induced BLG, would reduce the internal stress of crystals and thereby affect dislocation creep flow laws in regime 1. Therefore "DRX creep," as proposed by *Platt and Behr* [2011], may be effective in reducing the flow stress. At lower temperatures, close to the brittle–plastic transition zone (or semibrittle zone), power law breakdown occurs, and the rate of dislocation creep would be controlled by dislocation glide according to the Peierls mechanism [*Goetze*, 1978; *Poirier*, 1985]. Glide-controlled dislocation creep with an exponential flow law would then be activated; however, the occurrence of this type of creep has not been established for either dry or wet quartz.

A recent numerical study of shear zone development by *Moore and Parsons* [2015] demonstrated that shear zone width, w, is scaled by the stress exponent of power law creep as $w \sim n^{-1/2}$. Therefore, if pipe-diffusion-controlled dislocation creep is dominant around the brittle–plastic transition of quartz in nature, its large stress exponent ($n = 5$) may have important geophysical implications for strain localization and shear zone formation under the conditions of the upper to middle crust. Currently, there remain large uncertainties in flow law parameters at low temperatures. Hence, a dominance of volume-diffusion-controlled dislocation creep with a power of 3 in the lower-middle crust cannot be ruled out, and the simultaneous occurrence of other mechanisms such as DDRX and exponential creep in the upper to middle crust is also plausible.

Under the conditions of the brittle-plastic transition zone, microcracking likely occurs and crack tips become additional sources of dislocation formation [*Weertman*, 1981]. In such cases, dislocation densities would become much higher than those calculated from dislocation theory, possibly enhancing the contribution of pipe diffusion to the total diffusion [*Yund et al.*, 1981]. Whether or not pipe diffusion enhances climb-controlled dislocation creep in the middle to upper crust depends on the competing effects of increasing dislocation density and decreasing temperature. Microcracking and high dislocation densities are characteristics of experimentally deformed quartzite in the semibrittle flow regime of *Hirth and Tullis* [1994]. However, as the samples deformed by semibrittle flow showed only limited recovery, microcrack propagation associated with stress relaxation by dislocation glide was considered the dominant deformation process in this regime. Further studies combining theoretical and experimental approaches with field observations are needed to clarify the dislocation creep mechanisms in naturally deforming quartz.

6. Conclusions

Experimental data for quartz dislocation creep were compared with theories, which include creep that is controlled either by volume diffusion or pipe diffusion. Based on the similarities of the activation energies and dependencies on water fugacity in the dislocation creep experiments, we have considered oxygen-bearing volume diffusion along different crystallographic directions in α-quartz and β-quartz as well as pipe diffusion. Many experiments have been performed in the β-quartz field, and the raw experimental data are consistent with those calculated from theory with volume diffusion in β-quartz. In other words, the theories perform well in explaining the experimental data. Under natural conditions, water fugacity and differences in the strengths of α-quartz and β-quartz need to be considered when experimental flow laws are applied to naturally deformed α-quartz. To properly evaluate the influence of the α–β transition on the rheology of quartz, more experimental data for the α-quartz stability field are required. Dislocation creep controlled by pipe diffusion dominates at low temperatures under natural conditions, and it may be difficult to perform experiments involving dislocation creep that is controlled by pipe diffusion. This type of creep explains the microstructural changes reported at ~400°C fairly well and provides reasonable stress estimates at the brittle-plastic transition temperature of quartz rocks (around 300°C) under natural strain rates.

Appendix A

A1. Recalculation of the Flow Law of *Luan and Paterson* [1992]

Luan and Paterson [1992] reported a stress exponent of 4 and an activation energy of 152 kJ/mol for quartzite synthesized from silicic acid. They also reported on the deformation behavior of sintered natural quartz and quartz originating from a silica gel. The data for natural quartz are limited, and the measured differential stresses are mostly higher than 1000 MPa, which is much higher than the confining pressure of 300 MPa, thus leading to the development of fractures. *Luan and Paterson*'s [1992] data for silica gel quartz may include the effects of melt, which could reduce the stress exponent to ~2.3. Consequently, we did not use the data

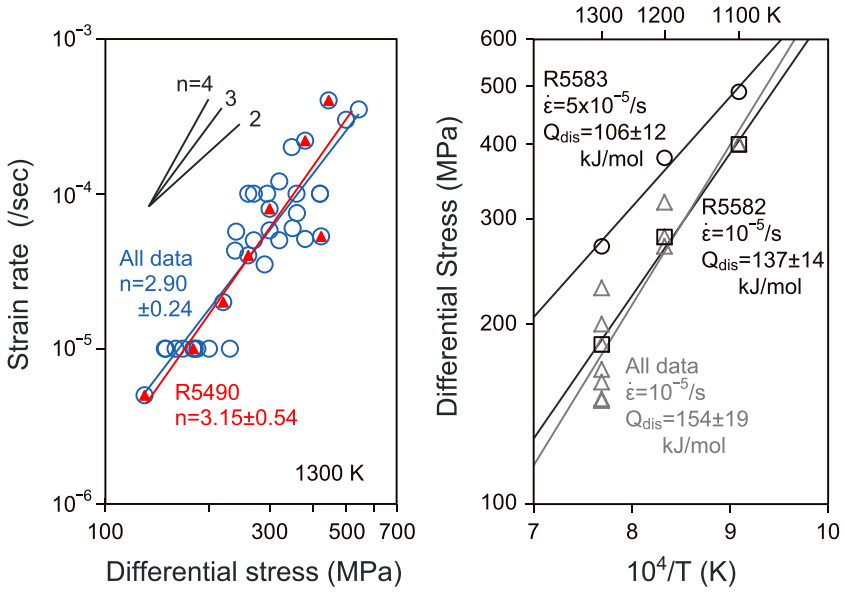

Figure A1. Determination of (left) stress exponents and (right) activation energies from the original data in *Luan and Paterson* [1992] for quartz aggregates that are synthesized from silicic acid. The red triangles on the left figure are from the strain rate stepping experiment at 1300 K (run 5490). The open blue squares are from all data at 1300 K. Activation energies on the right figure are calculated from the slopes of regression lines with a stress exponent of $n = 3$. Two temperature stepping experiments at constant strain rates (black open squares for run 5582 at $\dot{\varepsilon} = 10^{-5}$ s^{-1} and black open circles for run 5583 at $\dot{\varepsilon} = 5 \times 10^{-5}$ s^{-1}) and all data from different temperatures at $\dot{\varepsilon} = 10^{-5}$ s^{-1} (gray open triangles).

obtained for the sintered quartz and gel-origin samples. The flow law parameters for samples originating from silicic-acid, as defined by *Paterson and Luan* [1990], are listed in Table 1. However, they did not show the method of parameter fitting in a reproducible way. We therefore recalibrate the flow law using the experimental data of *Luan and Paterson* [1992]. The procedure was as follows.

Based on equation (2), the strain rate-stress relationship fixing other parameters can be written as

$$\Delta \ln \dot{\varepsilon} = n \Delta \ln \sigma. \tag{A1}$$

Thus, the stress exponent can be determined. Similarly, the stress-temperature relationship is

$$\Delta \ln \sigma = \frac{Q_{dis}}{Rn} \left(\Delta \frac{1}{T} \right). \tag{A2}$$

By applying the stress exponent from equation (A1), the activation energy is determined. Then, all parameters are substituted into equation (2) and the preexponential factor is determined. We use the averaged preexponential factor for the flow law.

The results are shown in Figure A1. The strain rate stepping experiment and all of the strain rate-stress data from *Luan and Paterson* [1992] gave a stress exponent of ~3, which differs from that given in the original paper. The stress-temperature relationships for all data are scattered, especially at 1300 K. Consequently, we used the data from their temperature stepping tests in runs 5582 and 5583. The sample in run 5582 had a water content of 460 ppm H/Si (70 ppm H_2O) at the end of the experimental run, as determined by IR spectroscopy using the calibration of *Paterson* [1982], whereas the sample in run 5583 contained 4600 ppm H/Si water (700 ppm H_2O). Assuming $n = 3$, the activation energies of creep in runs 5582 and 5583 were determined to be 137 and 106 kJ/mol, respectively. The higher water content in run 5583 contributes to reducing the activation energy. The averaged activation energy is 121 kJ/mol. Consequently, the A values determined are $10^{-7.58 \pm 0.43}$ MPa^{-n} s^{-1} from the strain rate stepping test (run 5490) with Q_{dis} = 121 kJ/mol and $10^{-6.83 \pm 0.60}$ MPa^{-n} s^{-1} from the temperature stepping tests (runs 5582 and 5583) with $n = 3$. These values are not very different, and we therefore apply an average value of $A = 10^{-7.20 \pm 0.52}$ MPa^{-n} s^{-1} for the revised flow law in Table 1. The representative water fugacity value under their experimental conditions is 280 MPa (Table 1), which means that A' is $10^{-9.65}$ MPa^{-n-r} s^{-1} with $r = 1$ from equation (3).

Acknowledgments
Special thanks go to A. Kronenberg for encouragement and useful comments. We also thank T. Okudaira, D. Sparks, and H. Nagahama for useful discussions. Reviews by J. Platt, W. Behr, and J. Muto are gratefully acknowledged. J.F. was supported financially by a Japan Society for the Promotion of Science (JSPS) Postdoctoral Fellowship for Research Abroad. This work was supported by a Grant-in-Aid for Scientific Research on Innovative Areas (KAKENHI 26109005 and 15K21755) from the Ministry of Education, Culture, Sports, Science, and Technology (MEXT). The data for this paper are available by contacting the corresponding author, JF at jfukuda@eps.s.u-tokyo.ac.jp.

References

Baëta, R. D., and K. H. G. Ashbee (1969), Slip systems in quartz: I. Experiments, *Am. Mineral.*, *54*, 1551–1573.
Behr, W. M., and J. P. Platt (2014), Brittle faults are weak, yet the ductile middle crust is strong: Implications for lithospheric mechanics, *Geophys. Res. Lett.*, *41*, 8067–8075, doi:10.1002/2014GL061349.
Béjina, F., and O. Jaoul (1996), Silicon self-diffusion in quartz and diopside measured by nuclear micro-analysis methods, *Phys. Earth Planet. Int.*, *97*, 145–162.
Boutonnet, E., P. H. Leloup, C. Sassier, V. Gardien, and Y. Ricard (2013), Ductile strain rate measurements document long-term strain localization in the continental crust, *Geology*, *41*, 819–822.
Chernak, L. J., G. Hirth, J. Selverstone, and J. Tullis (2009), Effect of aqueous and carbonic fluids on dislocation creep strength of quartz, *J. Geophys. Res.*, *114*, B04201, doi:10.1029/2008JB005884.
Cordier, P., B. Boulogne, and J. C. Doukhan (1988), Water precipitation and diffusion in wet quartz and wet berlinite $AlPO_4$, *Bull. Minéral.*, *111*, 113–137.
de Bresser, J. H. P., C. J. Peach, J. P. J. Reijs, and C. J. Spiers (1998), On dynamic recrystallization during solid state flow: Effects of stress and temperature, *Geophys. Res. Lett.*, *25*, 3457–3460, doi:10.1029/98GL02690.
de Bresser, J. H. P., J. H. Ter Heege, and C. J. Spiers (2001), Grain size reduction by dynamic recrystallization: Can it result in major rheological weakening?, *Int. J. Earth Sci.*, *90*, 28–45.
Epelboin, Y., and J. R. Patel (1982), Determination of Burgers vectors of dislocations in synthetic quartz by computer simulation, *J. Appl. Phys.*, *53*, 271–275.
Evans, H. E., and G. Knowles (1977), A model of creep in pure materials, *Acta Metall.*, *25*, 963–975.
Farver, J. R., and R. A. Yund (1991), Oxygen diffusion in quartz: Dependence on temperature and water fugacity, *Chem. Geol.*, *90*, 55–70.
Giletti, B. J., and R. A. Yund (1984), Oxygen diffusion in quartz, *J. Geophys. Res.*, *89*, 4039–4046, doi:10.1029/JB089iB06p04039.
Gleason, G. C., and J. Tullis (1995), A flow law for dislocation creep of quartz aggregates determined with the molten salt cell, *Tectonophysics*, *247*, 1–23.
Goetze, C. (1978), The mechanism of creep in olivine, *Philos. Trans. R. Soc. London, Ser. A*, *288*, 99–119.
Griggs, D. T. (1974), A model of hydrolytic weakening in quartz, *J. Geophys. Res.*, *79*, 1653–1661, doi:10.1029/JB079i011p01653.
Griggs, D. T., and J. D. Blacic (1965), Quartz: Anomalous weakness of synthetic crystals, *Science*, *147*, 292–295.
Hier-Majumder, S., S. Mei, and D. L. Kohlstedt (2005), Water weakening of clinopyroxenite in diffusion creep, *J. Geophys. Res.*, *110*, B07406, doi:10.1029/2004JB003414.
Hirth, G., and D. L. Kohlstedt (2015), The stress dependence of olivine creep rate: Implications for extrapolation of lab data and interpretation of recrystallized grain size, *Earth Planet. Sci. Lett.*, *418*, 20–26.
Hirth, G., and J. Tullis (1992), Dislocation creep regimes in quartz aggregates, *J. Struct. Geol.*, *14*, 145–159.
Hirth, G., and J. Tullis (1994), The brittle-plastic transition in experimentally deformed quartz aggregates, *J. Geophys. Res.*, *99*(B6), 11,731–11,747, doi:10.1029/93JB02873.
Hirth, G., C. T. Teyssier, and W. J. Dunlap (2001), An evaluation of quartzite flow laws based on comparisons between experimentally and naturally deformed rocks, *Int. J. Earth Sci.*, *90*, 77–87.
Holyoke, C. W., and A. K. Kronenberg (2010), Accurate differential stress measurement using molten salt cell and solid salt assemblies in the Griggs apparatus with applications to strength, parameters and rheology, *Tectonophysics*, *494*, 17–31, doi:10.1016/j.tecto.2010.08.001.
Holyoke, C. W., III, and A. K. Kronenberg (2013), Reversible water weakening of quartz, *Earth Planet. Sci. Lett.*, *374*, 185–190.
Huang, M. L., L. Wang, and C. M. L. Wu (2002), Creep behavior of eutectic Sn–Ag lead-free solder alloy, *J. Mater. Res.*, *17*, 2897–2903.
Jaoul, O., J. Tullis, and A. Kronenberg (1984), The effect of varying water contents on the creep behavior of Hevitree quartzite, *J. Geophys. Res.*, *B89*, 4298–4312, doi:10.1029/JB089iB06p04298.
Jung, H., I. Katayama, Z. Jiang, T. Hiraga, and S. Karato (2006), Effect of water and stress on the lattice-preferred orientation of olivine, *Tectonophysics*, *421*, 1–22.
Karato, S., and H. Jung (2003), Effects of pressure on high-temperature dislocation creep in olivine, *Philos. Mag.*, *83*, 401–414.
Kirby, S. H. (1977), The effect of the α–β transformation on the creep properties of hydrolytically-weakened synthetic quartz, *Geophys. Res. Lett.*, *4*, 97–100, doi:10.1029/GL004i003p00097.
Kirby, S. H., and J. W. McCormick (1979), Creep of hydrolytically-weakened synthetic quartz crystals orientated to promote {2110} $<$0001$>$ slip: A brief summary of work to date, *Bull. Minéral.*, *102*, 124–137.
Koch, P. S., J. M. Christie, A. Ord, and R. P. George Jr. (1989), Effect of water on the rheology of experimentally deformed quartzite, *J. Geophys. Res.*, *94*, 13,975–13,996, doi:10.1029/JB094iB10p13975.
Kohlstedt, D. L. (2006), The role of water in high-temperature rock deformation, *Rev. Mineral. Geochem.*, *62*, 377–396.
Kohlstedt, D. L., B. Evans, and S. J. Mackwell (1995), Strength of the lithosphere: Constraints imposed by laboratory experiments, *J. Geophys. Res.*, *100*, 17,587–17,602, doi:10.1029/95JB01460.
Kronenberg, A. K. (1994), Hydrogen speciation and chemical weakening of quartz, *Rev. Mineral. Geochem.*, *29*, 123–176.
Kronenberg, A. K., and J. Tullis (1984), Flow strengths of quartz aggregates: Grain size and pressure effects due to hydrolytic weakening, *J. Geophys. Res.*, *89*, 4281–4297.
Legros, M., G. Dehm, E. Arzt, and T. J. Balk (2008), Observation of giant diffusivity along dislocation cores, *Science*, *319*, 1646–1649.
Linker, M. F., and S. H. Kirby (1981), Anisotropy of the rheology of hydrolytically weakened synthetic quartz crystals, *Geophys. Monogr. Ser.*, *24*, 29–48.
Linker, M. F., S. H. Kirby, A. Ord, and J. M. Christie (1984), Effects of compression direction on the plasticity and rheology of hydrolytically weakened synthetic quartz crystals at atmospheric pressure, *J. Geophys. Res.*, *89*, 4241–4255, doi:10.1029/JB089iB06p04241.
Lister, G. S. (1981), The effect of the basal–prism mechanism switch on fabric development during plastic deformation, *J. Struct. Geol.*, *3*, 67–75.
Lister, G. S., M. S. Paterson, and B. E. Hobbs (1978), The simulation of fabric development in plastic deformation and its application to quartzite: The model, *Tectonophysics*, *45*, 107–158.
Luan, F. C., and M. S. Paterson (1992), Preparation and deformation of synthetic aggregates of quartz, *J. Geophys. Res.*, *B97*, 301–320, doi:10.1029/91JB01748.
Luthy, H., A. K. Miller, and O. D. Sherby (1980), The stress and temperature dependence of steady-state flow at intermediate temperatures for pure polycrystalline aluminum, *Acta Metall.*, *28*, 169–178.
Mainprice, D., J. L. Bouchez, P. Blumenfeld, and J. M. Tubià (1986), Dominant *c* slip in naturally deformed quartz: Implications for dramatic plastic softening at high temperature, *Geology*, *14*, 819–822.

Mathew, M. D., H. Yang, S. Movva, and K. L. Murty (2005), Creep deformation characteristics of tin and tin-based electronic solder alloys, *Metall. Mater. Trans.*, *A36*, 99–105.
McLaren, A. C., J. D. Fitz Gerald, and J. Gerretsen (1989), Dislocation nucleation and multiplication in synthetic quartz: Relevance to water weakening, *Phys. Chem. Miner.*, *16*, 465–482.
Mei, S., and D. L. Kohlstedt (2000a), Influence of water on plastic deformation of olivine aggregates 1. Diffusion creep regime, *J. Geophys. Res.*, *105*(B9), 21,457–21,469, doi:10.1029/2000JB900179.
Mei, S., and D. L. Kohlstedt (2000b), Influence of water on plastic deformation of olivine aggregates 2. Dislocation creep regime, *J. Geophys. Res.*, *105*(B9), 21,471–21,481, doi:10.1029/2000JB900180.
Menegon, L., P. Nasipuri, H. Stünitz, H. Behrens, and E. Ravna (2011), Dry and strong quartz during deformation of the lower crust in the presence of melt, *J. Geophys. Res.*, *116*, B10410, doi:10.1029/2011JB008371.
Moore, J. D. P., and B. Parsons (2015), Scaling of viscous shear zones with depth-dependent viscosity and power-law stress-strain-rate dependence, *Geophys. J. Int.*, *202*, 242–260.
Okudaira, T., and N. Shigematsu (2012), Estimates of stress and strain rate in mylonites based on the boundary between the fields of grain-size sensitive and insensitive creep, *J. Geophys. Res.*, *117*, B03210, doi:10.1029/2011JB008799.
Parrish, D. K., A. L. Krivz, and N. L. Carter (1976), Finite-element folds of similar geometry, *Tectonophysics*, *32*, 183–207.
Paterson, M. S. (1982), The determination of hydroxyl by infrared absorption in quartz, silicate glasses and similar materials, *Bull. Minéral.*, *105*, 20–29.
Paterson, M. S. (1989), The interaction of water with quartz and its influence in dislocaiton flow-an over view, in *Rheology of Solids and of the Earth*, edited by S. Karato and M. Toriumi, pp. 107–142, Oxford Univ. Press, Oxford.
Paterson, M. S., and F. C. Luan (1990), Quartzite rheology under geological conditions, *Geol. Soc. Spec. Publ.*, *54*, 299–307.
Pitzer, K. S., and S. M. Sterner (1994), Equations of state valid continuously from zero to extreme pressures for H_2O and CO_2, *J. Chem. Phys.*, *101*, 3111–3116.
Platt, J. P., and W. M. Behr (2011), Grainsize evolution in ductile shear zones: Implications for strain localization and the strength of the lithosphere, *J. Struct. Geol.*, *33*, 537–550.
Poirier, J. P. (1985), *Creep of Crystals: High-Temperature Deformation Process in Metals, Ceramics and Minerals*, Cambridge Univ., Cambridge, U. K.
Post, A., J. Tullis, and R. A. Yund (1996), Effects of chemical environment on dislocation creep of quartzite, *J. Geophys. Res.*, *101*(B10), 22,143–22,155, doi:10.1029/96JB01926.
Ruano, O. A., A. K. Miller, and O. D. Sherby (1981), The influence of pipe diffusion on the creep of fine-grained materials, *Mater. Sci. Eng.*, *51*, 9–16.
Rutter, E. H., and K. H. Brodie (2004a), Experimental intracrystalline plastic flow in hot-pressed synthetic quartzite prepared from Brazilian quartz crystals, *J. Struct. Geol.*, *26*, 259–270.
Rutter, E. H., and K. H. Brodie (2004b), Experimental grain-size sensitive flow of hot-pressured Brazilian quartz aggregates, *J. Struct. Geol.*, *26*, 2011–2023.
Rybacki, E., M. Gottschalk, R. Wirth, and G. Dresen (2006), Influence of water fugacity and activation volume on the flow properties of fine-grained anorthite aggregates, *J. Geophys. Res.*, *111*, B03203, doi:10.1029/2005JB003663.
Shimizu, I. (1998), Stress and temperature dependence of recrystallized grain size: A subgrain misorientation model, *Geophys. Res. Lett.*, *22*, 4237–4240, doi:10.1029/1998GL900136.
Shimizu, I. (2008), Theories and applicability of grain size piezometers: The role of dynamic recrystallization mechanisms, *J. Struct. Geol.*, *30*, 899–917.
Shimizu, I. (2011), Erratum to "Theories and applicability of grain size piezometers: The role of dynamic recrystallization mechanisms" [*J. Struct. Geol.* 30 (2008), 899–917], *J. Struct. Geol.*, *33*, 1136–1137.
Shimizu, I. (2012), Steady-state grain size in dynamic recrystallization of minerals, in *Recrystallization*, edited by K. Sztwiertnia, pp. 371–386, InTech, Rijeka, Croatia. [Available at http://www.intechopen.com/books/recrystallization/.]
Shimizu, I. (2014), Rheological profile across the NE Japan interplate megathrust in the source region of the 2011 M_w9.0 Tohoku-oki earthquake, *Earth Planets Space*, *66*, 73.
Somekawa, H., K. Hirai, H. Watanabe, Y. Takigawa, and K. Higashi (2005), Dislocation creep behavior in Mg–Al–Zn alloys, *Mater. Sci. Eng.*, *A407*, 53–61.
Spingarn, J. R., D. M. Barnett, and W. D. Nix (1979), Theoretical descriptions of climb controlled steady state creep at high and intermediate temperatures, *Acta Metall.*, *27*, 1549–1561.
Sterner, S. M., and K. S. Pitzer (1994), An equation of state for carbon dioxide valid from zero to extreme pressures, *Contrib. Mineral. Petrol.*, *117*, 362–374.
Stipp, M., H. Sünitz, R. Heilbronner, and S. M. Schmid (2002a), The eastern Tonale fault zone: A 'natural laboratory' for crystal plastic deformation of quartz over a temperature range from 250 to 700 °C, *J. Struct. Geol.*, *24*, 1861–1884.
Stipp, M., H. Sünitz, R. Heilbronner, and S. M. Schmid (2002b), Dynamic recrystallization of quartz: Correlation between natural and experimental conditions, in *Deformation Mechanisms, Rheology and Tectonics: Current Status and Future Perspectives*, *Geol. Soc. Spec. Publ*, edited by D. De Meer et al., pp. 170–190.
Stipp, M., and J. Tullis (2003), The recrystallized grain size piezometer for quartz, *Geophys. Res. Lett.*, *30*(21), 2088, doi:10.1029/2003GL018444.
Stipp, M., J. Tullis, and H. Behrens (2006), Effect of water on the dislocation creep microstructure and flow stress of quartz and implications for the recrystallized grain size piezometer, *J. Geophys. Res.*, *111*, B04201, doi:10.1029/2005JB003852.
Takeshita, T., and H.-R. Wenk (1988), Plastic anisotropy and geometrical hardening in quartzites, *Tectonophysics*, *149*, 345–361.
Trepied, L., and J. C. Doukhan (1978), Dissociated 'a' dislocations in quartz, *J. Mater. Sci.*, *13*, 492–498.
Twiss, R. J. (1977), Theory and applicability of recrystallized grain size paleopiezometer, *Pure Appl. Geophys.*, *115*, 227–244.
Weertman, J. (1955), Theory of steady-state creep based on dislocation climb, *J. Appl. Phys.*, *26*, 1213–1217.
Weertman, J. (1970), The creep strength of the Earth's mantle, *Rev. Geophys. Space Phys.*, *26*, 145–168.
Weertman, J. (1981), Crack tip blunting by dislocation pair creation and separation, *Philos. Mag. A*, *43*, 1103–1123.
Wightman, R. H., D. J. Prior, and T. A. Little (2006), Quartz veins deformed by diffusion creep-accommodated grain boundary sliding during a transient, high strain-rate event in the Southern Alps, New Zealand, *J. Struct. Geol.*, *28*, 902–918.
Yund, R. A., B. M. Smith, and J. Tullis (1981), Dislocation-assisted diffusion of oxygen in albite, *Phys. Chem. Miner.*, *7*, 185–189.